Earth Surface Processes and Landforms
Earth Surf. Process. Landforms **30**, 1597–1615 (2005)
Published online in Wiley InterScience (www.interscience.wiley.com). **DOI:** 10.1002/esp.1234

Defining the moment of erosion: the principle of thermal consonance timing

D. M. Lawler*
School of Geography, Earth and Environmental Sciences, The University of Birmingham, Birmingham B15 2TT, UK

**Correspondence to:*
D. M. Lawler, School of Geography, Earth and Environmental Sciences, University of Birmingham, Birmingham B15 2TT.
E-mail: D.M.Lawler@bham.ac.uk

Abstract

Geomorphological process research demands quantitative information on erosion and deposition event timing and magnitude, in relation to fluctuations in the suspected driving forces. This paper establishes a new measurement principle – thermal consonance timing (TCT) – which delivers clearer, more continuous and quantitative information on erosion and deposition event magnitude, timing and frequency, to assist understanding of the controlling mechanisms. TCT is based on monitoring the switch from characteristically strong temperature gradients in sediment, to weaker gradients in air or water, which reveals the moment of erosion. The paper (1) derives the TCT principle from soil micrometeorological theory; (2) illustrates initial concept operationalization for field and laboratory use; (3) presents experimental data for simple soil erosion simulations; and (4) discusses initial application of TCT and perifluvial micrometeorology principles in the delivery of timing solutions for two bank erosion events on the River Wharfe, UK, in relation to the hydrograph.

River bank thermal regimes respond, as soil temperature and energy balance theory predicts, with strong horizontal thermal gradients (often >1 K cm^{-1} over 6·8 cm). TCT fixed the timing of two erosion events, the first during inundation, the second 19 h after the discharge peak and 13 h after re-emergence from the flow. This provides rare confirmation of delayed bank retreat, quantifies the time-lag involved, and suggests mass failure processes rather than fluid entrainment. Erosion events can be virtually instantaneous, implying 'catastrophic retreat' rather than 'progressive entrainment'. Considerable potential exists to employ TCT approaches for: validating process models in several geomorphological contexts; assisting process identification and improving discrimination of competing hypotheses of process dominance through high-resolution, simultaneous analysis of erosion and deposition events and driving forces; defining shifting erodibility and erosion thresholds; refining dynamic linkages in event-based sediment budget investigations; and deriving closer approximations to 'true' erosion and deposition rates, especially in self-concealing scour-and-fill systems. Copyright © 2005 John Wiley & Sons, Ltd.

Received 28 April 2004;
Revised 19 July 2004;
Accepted 21 March 2005

Keywords: bank erosion event; river bank temperature; soil temperature gradient; PEEP-3 sensor; mass failure; perifluvial micrometeorology

Introduction

The need to integrate reliable information on erosion and deposition event timing and magnitude when deciphering geomorphological processes is paramount. A number of supportive arguments for this position have been advanced in geomorphology (e.g. Church, 1980, 1996; Lawler, 1991, 1992, 1994, 2005; Richards, 1996; Lane, 1998; Lane *et al.*, 1998a; Casadei *et al.*, 2003; Hall, 2004) and in other scientific disciplines, including cognate ones such as oceanographic or coastal sciences (e.g. Morris *et al.*, 2001; Ridd *et al.*, 2001; Betteridge *et al.*, 2003). The arguments largely pertain to the need to determine, at the appropriate scales of space and time, the magnitude and timing of geomorphological change in relation to variations in the stresses applied by suspected driving forces. For example, Richards (1996, p. 176) argues that 'intensive research frequently demands study of interaction and coincidence, and therefore is crucially dependent on simultaneous study of several related phenomena and processes'.

Moreover, because in many geomorphological systems erosion is achieved in discrete, episodic events, it is the details of individual event structure (e.g. slow and progressive or catastrophic and instantaneous) and temporal distribution that are often of most interest. This includes information on the *singular* erosion event, principally magnitude, rate-change, timing and duration (i.e. response dynamics), which will also allow the capture of the *collective* details of event return frequency, combination, sequencing and juxtaposition. This provides a reasonable basis for the identification and quantification of processes, including changing patterns of relative dominance when multiple candidate processes are at work.

In particular, erosion event timing information would help to clarify: (1) threshold operation, including transient threshold shifts (e.g. critical entrainment values in relation to sediment erodibility changes), time-dependent behaviour and non-linearities; (2) time-lags between stress application and geomorphological response, which may reveal much about process mechanics and the presence of secondary or tertiary processes; (3) the role of antecedent conditions (e.g. Lau and Droppo, 2000), not least because the temporal boundaries of the antecedent period would be established more certainly; (4) event precedence details as an aid to process exclusion, given that current events cannot drive previous erosion (though, equally, temporal coincidence is no guarantee of causality); (5) erosion rates, which are closer to the 'true' values than temporally lumped estimates. This is especially important in self-concealing systems such as scour-and-fill environments (e.g. tidal or semi-arid channels); (6) links with derivative processes, such as stream sediment flux perturbations following injection of material from a discrete erosional event; (7) the building, calibration and validation of erosion and sediment transport models of high spatial and temporal resolution (e.g. Bates and Lane, 2000; Mosselman, 2000).

Erosion and deposition monitoring, however, has often been achieved through periodic manual resurvey techniques based on, for example, erosion pins, total stations, GPS, repeat imaging, terrestrial photogrammetry, aerial photogrammetry, serial cartography and remote sensing (see Lawler (1993a), Lawler *et al.* (1997a), Lane *et al.* (1998b) and Simon and Castro (2003) for reviews). Newer developments, in particular, have emerged with terrestrial photogrammetric approaches (e.g. Lawler, 1989, 1993a; Lane *et al.*, 1993, 1998a; Barker *et al.*, 1997; Westaway *et al.*, 2000; Brasington *et al.*, 2003). However, although some automated methods for quasi-continuous qualitative or semi-quantitative monitoring have emerged recently, further progress is desirable to facilitate the routine capture of key event-specific details to assist process explanations. This would help to match recent developments in continuous bedload transport monitoring (e.g. Garcia *et al.*, 2000; Habersack *et al.*, 2001). The photo-electronic erosion pin (PEEP) system, for example (Lawler, 1991, 1992, 1994; Lawler *et al.*, 1997b), allows semi-continuous erosion and deposition data to be collected from a range of environments (e.g. Lawler *et al.*, 1997b, 2001; Couperthwaite *et al.*, 1998; Mitchell *et al.*, 1999, 2003; Stott, 1999; Prosser *et al.*, 2000) and has afforded fresh insights into erosion dynamics and processes. However, despite its advantages, the PEEP system incurs delays in the detection of nocturnal erosion events or intra-hydrograph activity because of low light levels at those times. There is a real need, therefore, for a technique which is truly continuous and appropriate for longer-term, routine capture of high-frequency geomorphological change data at the event timescale.

To help address this challenge, the aim of this paper is to discuss a new measurement principle – thermal consonance timing (TCT) – which delivers clearer, more continuous and quantitative information on erosion and deposition event magnitude, timing and frequency, with the potential to develop a better understanding of the driving processes. Specifically, the paper: (1) advances the TCT principle in the context of micrometeorological theory; (2) describes how the TCT concept has been made initially operational for use in the field and laboratory; (3) briefly presents experimental data from a very simple soil erosion simulation; (4) discusses in detail the success of applying the TCT principle to extract much clearer timing information for two example river bank erosion events; and (5) outlines the promise suggested by the TCT approach for explanation and model-testing in erosion process investigations more generally.

The Principle of Thermal Consonance Timing

The principle of TCT is developed to provide a method of determining the timing of erosion events. It should be applicable to many geomorphological systems (e.g. gullies, hillslopes, dunes, beaches, mudflats); for this paper, however, fluvial examples are presented to illustrate the principles, operation and potential of the concept. The TCT concept is based on the differences between temperature gradients developed in sediment or soil and those in air or water, and draws on energy balance and soil heat flux theory. This body of theory has rarely been applied to fluvial systems (but see Lawler, 1993b; Branson *et al.*, 1996; Evans *et al.*, 1998); moreover few river bank temperature data have been published (but see Lawler, 1987, 1992, 1993b; Stott, 1999) in comparison with other components of the fluvial system, such as stream water (e.g. Webb and Zhang, 1999), river beds (Evans *et al.*, 1998) and hyporheic zones

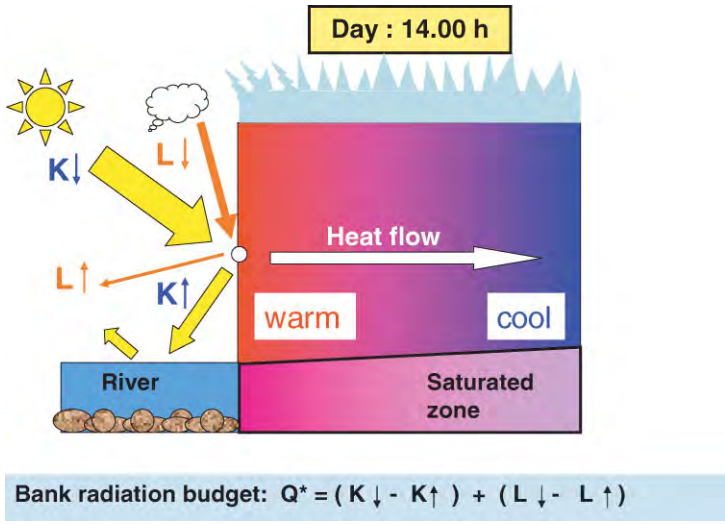

Figure 1. Perifluvial micrometeorology: daylight radiation budget terms for a river bank, with graphical representation of typical relative dominance of fluxes, thermal gradients and resultant heat flow direction. This figure is available in colour online at www.interscience.wiley.com/journal/espl

(Evans and Petts, 1997). The theory and published evidence are used here to establish a new geomorphological measurement principle, as part of what can be termed applied 'perifluvial micrometeorology' (Figure 1).

Perifluvial micrometeorology: radiation budgets and energy balances of river bank surfaces

The discussion here is cast in terms of river banks, though it is adaptable to many soil and sediment surfaces, and uses the terminology of Oke (1987) under idealized conditions. During daylight hours, river banks, much like their horizontal soil surface counterparts, receive short-wave solar and long-wave terrestrial radiation defined by the radiation budget (Figure 1):

$$Q^* = (\mathrm{K}\downarrow - \mathrm{K}\uparrow) + (\mathrm{L}\downarrow - \mathrm{L}\uparrow) \tag{1}$$

where Q^* is net all-wavelength radiation receipt, K↓ is incident solar short-wave radiation, K↑ is reflected solar short-wave radiation, L↓ is incident terrestrial long-wave radiation, and L↑ is reradiated terrestrial long-wave radiation. Much more short-wave radiation is normally received than is emitted by long-wave radiation (though some solar short-wave is reflected), and this net accumulation of radiant energy drives a warming of the bank surface (Figure 1). Heating rates depend on partitioning within the energy balance equation (e.g. Oke, 1987; Cellier *et al.*, 1996):

$$Q^* = Q_H + Q_E + Q_G + \Delta Q_S \tag{2}$$

where Q_H is sensible heat, Q_E is latent heat, Q_G is conduction to and from the underlying soil or sediment, and ΔQ_S is change in energy storage. In practice, however, energy transfer to depth in the sediment body is constrained, especially in coarse and/or dry materials with limited grain-to-grain thermal contact, resulting in strong thermal gradients (Oke, 1987), with much greater temperatures at the sediment surface than at depth (Figure 1). Heat flow, according to normal flux gradient relationships (e.g. Oke, 1987; Cellier *et al.*, 1996), takes place along the gradient from warm to cool zones (Figure 1).

However, at night (Figure 2), the radiation budget system simplifies, and Q^* declines, because solar radiation receipts are reduced to zero:

$$Q^* = (\mathrm{L}\downarrow - \mathrm{L}\uparrow) \tag{3}$$

Although some terrestrial long-wave radiation is received, the budget is dominated by long-wave outputs from the radiating sediment surface (Figure 2), which cools more than the interior. This establishes a reverse temperature gradient and heat flux towards the surface (Figure 2).

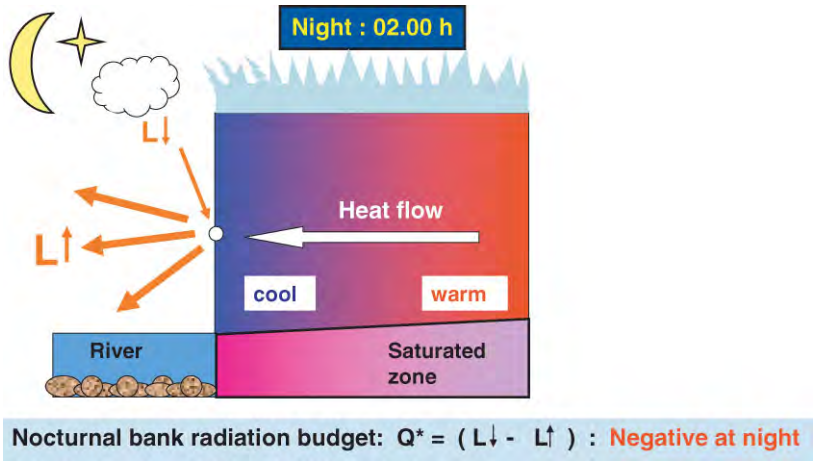

Figure 2. Perifluvial micrometeorology: nocturnal radiation budget terms for a river bank, with graphical representation of typical relative dominance of fluxes, thermal gradients and resultant heat flow direction. This figure is available in colour online at www.interscience.wiley.com/journal/espl

Sediment temperature cycles

As a result of these radiation budgets and energy balances, a significant diurnal cycle is established for sediment temperature (idealized in Figure 3A). However, changes to energy receipts and fluxes with depth set up different diurnal temperature cycling characteristics between the sediment surface and interior (Figure 3A). The key differences are: (1) the amplitude of diurnal temperature cycles is greater at the surface than at depth (see ΔT_{max}), with higher maxima and lower minima (e.g. Sinokrot and Stefan, 1993); and (2) a phase shift, Δt, in the times of the daily thermal peaks and troughs for the interior, which lag behind those for the sediment surface (Figure 3A), because of time lags in the downward transmission of the temperature wave conditioned by thermal diffusivity (thermal conductivity / heat capacity) (see Oke, 1987; Cellier *et al.*, 1996; Lantzke *et al.*, 1999). However, diurnal temperature cycle wavelengths are broadly similar at the surface and shallow depths (Figure 3A). A huge body of empirical evidence exists in the soil physics, boundary later meteorology, hydrology, agricultural climatology and engineering literature to confirm these features, collected across a range of soil and sediment types (including river beds), ground covers and climatic environments (e.g. Oke, 1987; Sinokrot and Stefan, 1993; Cellier *et al.*, 1996; Evans and Petts, 1997; Lantzke *et al.*, 1999; Ogée *et al.*, 2001; Ogée and Brunet, 2002; Kumar and Kaleita, 2003). Indeed, soil thermal profiles are used to calibrate and validate heat flux models (e.g. Sinokrot and Stefan, 1993). Empirical evidence in Figure 3B shows that these effects are also common at subseasonal and seasonal timescales. Note that thermal amplitude successively decreases, and peak and trough lags tend to increase, with depth below the river bed (Figure 3B) (see also Oke, 1987; Evans and Petts, 1997). Furthermore, results below indicate that river bank thermal regimes tend to operate in much the same way as surface soils and river beds.

Thus, around midday, temperatures are classically high at the sediment surface (the radiation exchange surface) but decline strongly with depth, z, often at a logarithmic rate (Oke, 1987) (Figure 4A): this is supported by substantial evidence (e.g. Figure 4B: Ogée *et al.*, 2001). Such temperature gradients are maximized under conditions of strong insolation, and in dry and coarse materials, and Figure 4B demonstrates the considerable impact of early morning warming on the upper few centimetres of soil temperature profiles. Although there is often a decline in air temperature with height, z, above the surface, as shown in the schematic lapse profile of Figure 4A discussed in detail by Oke (1987), it is well documented that soil or sediment temperature gradients are generally stronger than in the adjacent air or flowing water (e.g. Oke, 1987; Sinokrot and Stefan, 1993; Cellier *et al.*, 1996; Kumar and Kaleita, 2003). This is because heat transfers which redistribute energy through the overlying air or water column are considerably assisted by turbulent exchanges denied to the sediment body.

Using soil micrometeorological theory as an erosion measurement principle

Thus, a given space occupied by sediment or soil normally develops significant thermal gradients, with time-dependent magnitudes and directions. However, if erosion then removes that sediment, and replaces it with air or water, that

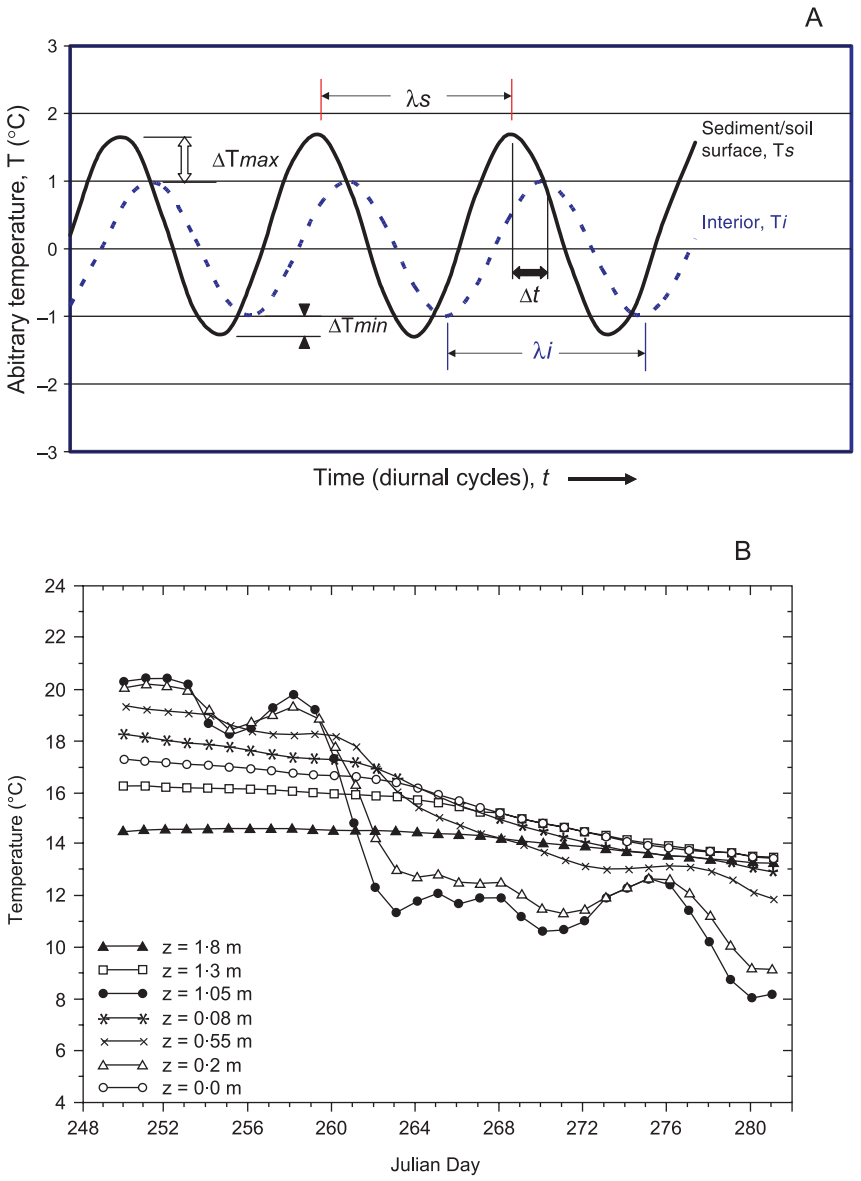

Figure 3. Temperature cycling of the sediment surface and at depth: (A) classic schematic diurnal sinusoidal curves; (B) temperature changes with depth at subseasonal timescales for the bed of the Rum River, Minnesota, USA, from the river bed surface (z = 0·0 m) to 1·8 m below the bed (from Sinokrot and Stefan, 1993). This figure is available in colour online at www.interscience.wiley.com/journal/espl

space becomes characterized by much weaker temperature gradients. Knowing the time of the sustained switch from strong to weak thermal gradients, therefore, permits the determination of the moment of erosion. This *sustained* thermal consonance should not be confused with the *transient* isothermal condition obtained fairly regularly in soils during thermal crossover (sometimes semi-diurnally), and related to differentials in energy exchanges and heating and cooling rates between the soil surface and subsurface (e.g. Figures 1–3). Conversely, if deposition occurs, stronger thermal gradients should be generated in the sedimentation space that replaces the water or air column.

A simple instrument equipped with thermistors, therefore, can be inserted into an eroding or depositing landform, as shown schematically in Figure 5, and attached to a datalogger. Subsequently, if erosion exposes the thermistors to air or water, temperature gradients are minimized and the thermistors will register virtually identical temperatures (Figures 4 and 5). Thus they achieve a condition of thermal consonance. The onset of sustained (near-) isothermal

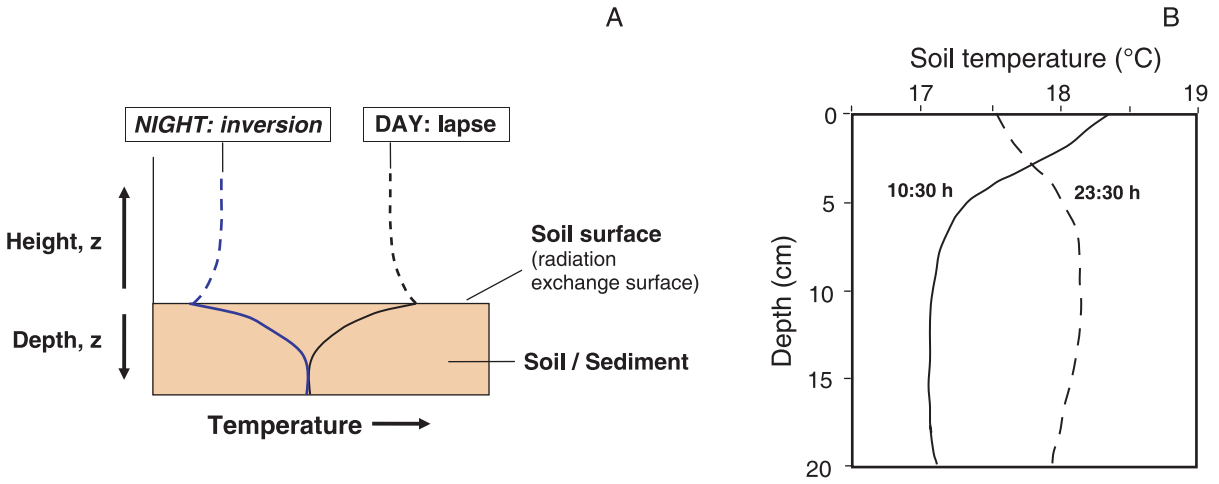

Figure 4. Vertical temperature gradients: (A) idealized daytime lapse profiles and nocturnal inversions in the near-surface sediment and air column from Oke (1987) (see also Cellier *et al.*, 1996), showing much stronger temperature gradients in soil than in the overlying air; (B) detailed morning and nocturnal temperature profiles measured in a sandy podzolic soil in a maritime pine stand near Bordeaux, France, September 1997 (Ogée *et al.*, 2001). This figure is available in colour online at www.interscience.wiley.com/journal/espl

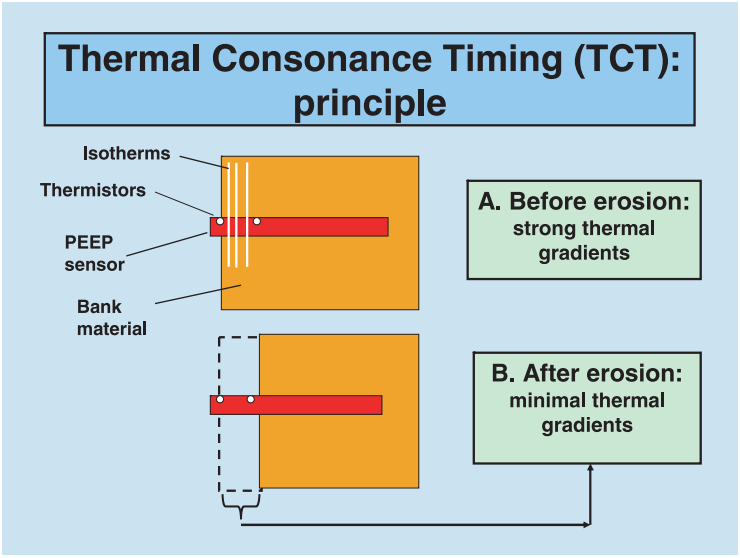

Figure 5. The principle of thermal consonance timing (TCT). Sediment bodies are normally characterized by strong temperature gradients: when sediment is removed by erosion, much weaker temperature gradients result. The principle should also work in reverse to allow automatic monitoring of deposition events and rates. This figure is available in colour online at www.interscience.wiley.com/journal/espl

conditions in the measurement space therefore represents the moment of erosion, namely the switch from sediment to air or water (Figure 5), and is the principle underpinning the concept of thermal consonance timing.

Making the TCT Concept Operational

For these experiments, the TCT concept was validated with initial instruments developed by simply adding two thermistors to existing photo-electronic erosion pin (PEEP) automatic erosion and deposition monitoring sensors

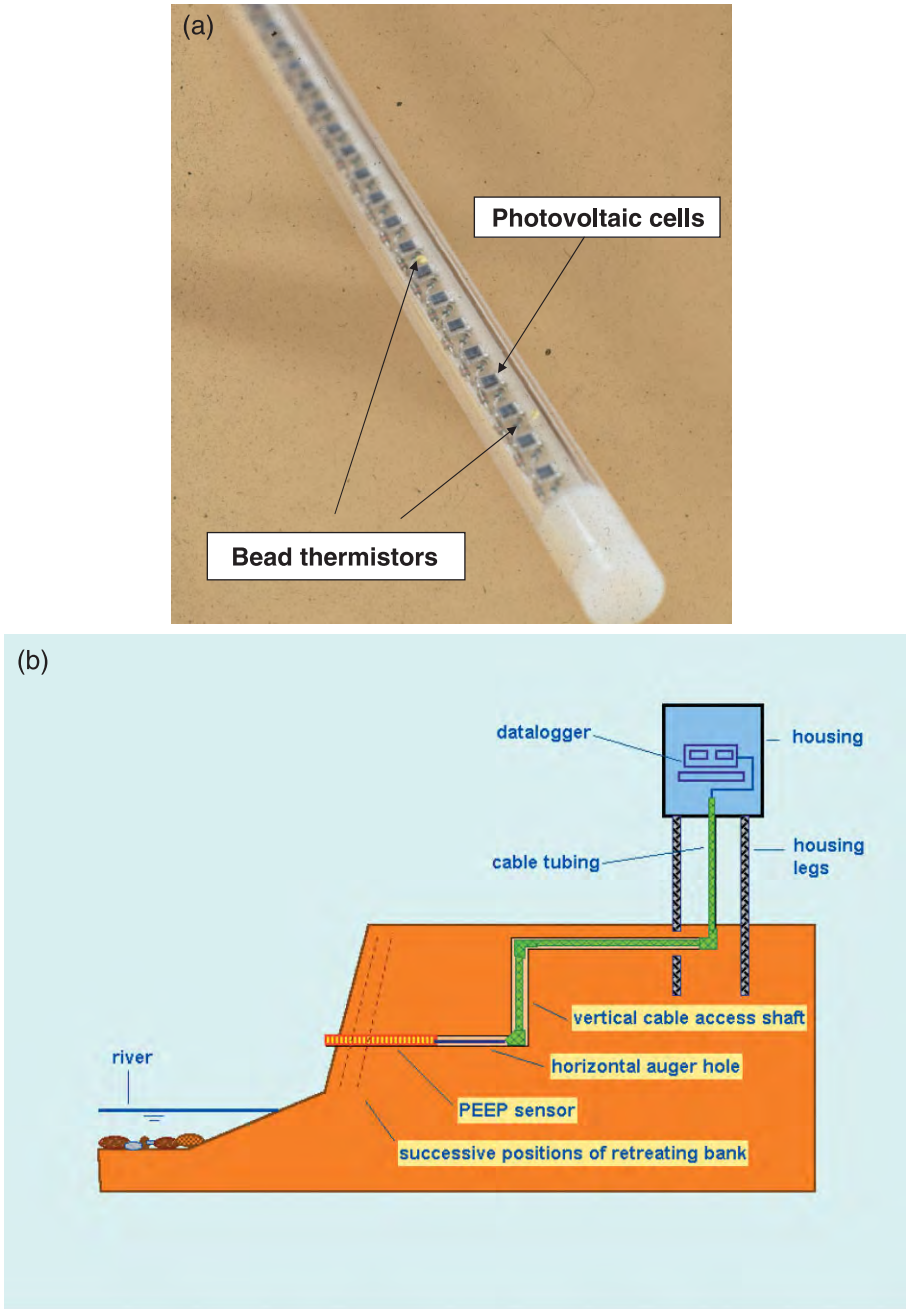

Figure 6. The PEEP-3 (photo-electronic erosion pin mark 3) sensor: (A) modified PEEP-3 sensor with two thermistors added near the front end of the photocell array; (B) typical installation for a river bank investigation (the scheme for the six PEEP-3 sensors per site used here was a grid network of three verticals with two sensors per vertical). This figure is available in colour online at www.interscience.wiley.com/journal/espl

(Lawler, 1991, 1992, 1994; Lawler *et al.*, 1997b; 2001). PEEP sensors are self-powering, analogue optoelectronic devices of 16 mm o.d. and 12 mm i.d. (Figure 6A), and responsive to visible and near-infra-red radiation, with peak spectral sensitivity at 920 nm. The instruments are installed into eroding or accreting landforms and connected to a datalogger (e.g. Figure 6B). Any subsequent erosion exposes more sensor to incident light which increases photovoltaic outputs from the cell series (*c.* 1 mV per 1 mm erosion), relative to the reference cells which allow normalization of the signal

for changing background light intensity. Depositional activity reduces photovoltaic outputs. Photovoltaic signals thus quantify erosional and depositional activity, especially the magnitude, frequency and timing of erosion and deposition events and rates, much more clearly than with manual methods, and this has led to significant improvements in understanding processes of river bank erosion (e.g. Lawler, 1994, Stott, 1999), canal stability (Prosser *et al.*, 2000) and tidal channels (Mitchell *et al.*, 1999; Lawler *et al.*, 2001). PEEP advantages and limitations are fully discussed elsewhere (e.g. Lawler, 1991, 1993a; Lawler *et al.*, 1997a, 2001). Despite being a significant improvement over manual monitoring systems, one limitation is that, being a light-dependent method, there is a delay in the detection of nocturnal events until the following morning when the PEEP sensor is reactivated.

Therefore, as part of a suite of improvements that resulted in the PEEP-3 instrument, and to conduct a field test of the TCT concept, two miniature, high-precision, low temperature-coefficient, low current-drain, 3 mm bead thermistors (Ketema-Rodan Accu-Curve ACC-004) were included on the printed circuit board inside a PEEP-3 sensor (Figure 6A). These negative temperature coefficient thermistors provide accurate and stable temperature sensing measurements: the manufacturer gives a tolerance for the devices of ±0·2 °C and a stability of ±0·1 °C per annum. For this study, thermistors were simply connected in series with a Campbell-Scientific CR10X datalogger which provided a low and very stable voltage supply with a sensitivity suitable for expected temperature differences. For future deployments, an even more sensitive method using a bridge circuit could be used, and for extremely sensitive temperature differential studies, two or more thermistors can be placed in the legs of bridge circuits: the manufacturer states that differentials as small as 0·001 °C can be detected this way. The thermistors were positioned between photocells near the front end of the PEEP-3 board to give an inter-thermistor separation of 68 mm (Figure 6A). Once connected to a datalogger, temperatures and temperature differences and gradients could be monitored continuously, in addition to normal light-based PEEP signals. It is stressed that, although for this proof-of-concept study two thermistors were used, sensors could include a very large number of thermistors, spanning a longer distance at a finer spatial resolution (e.g. <1 cm), to extend the applicability of the TCT principle to a wider range of sites and conditions.

Soil Temperature Experiment: A Simple Erosion Simulation

Brief results are first presented of simple tests carried out on temperature gradients within and above a bare patch of loosely structured, organic soil in south Warwickshire, UK, to provide a simple soil erosion simulation. The experimental design is shown in Figure 7, in which two PEEP-3 TCT sensors were established vertically alongside each other, one to record soil temperatures and gradients, the other to register air temperatures and gradients. This aimed to mimic a field situation following an erosion event which had exposed both thermistors (Figure 7). For comparative purposes, this concurrent approach obviated the difficulties posed by changing ambient conditions with a before-and-after strategy. Data are presented here for a week in early autumn (4–11 September 2003) which included a good range of conditions, including very hot, warm, overcast, misty and rainy periods. As theory and extensive soil temperature measurement programmes elsewhere would suggest (Oke, 1987; Cellier *et al.*, 1996; Ogée *et al.*, 2001), near-surface soil temperature differences here, whether positive or negative, were much greater than in the overlying air column (Figure 8). Vertical soil temperature differences across the 68 mm distance, z, ranged from −8·5 to +21·6 K, equating to soil thermal gradients, $\delta T_S/\delta z$, of −1·2 to 3·2 K cm^{-1} (Figure 8). Soil temperature gradients, on average, were almost ten times higher than air temperature gradients, $\delta T_A/\delta z$ (K cm^{-1}), as suggested by the coefficient in the simple linear least squares fit ($p < 0{\cdot}0001$) to the data of Figure 8:

$$\delta T_S/\delta z = 9{\cdot}9604\ (\delta T_A/\delta z) - 0{\cdot}303 \tag{4}$$

A positive gradient here implies higher temperatures at the sediment surface, and heat flow into the soil interior. As predicted, Figure 8 demonstrates that the distribution is asymmetric about the zero gradient line, with the range of positive temperature gradients (generated by surface warming from strong insolation) considerably greater than negative gradients (related to surface cooling).

Field Methods

Data are discussed from field experiments on the River Wharfe at Easedike, near Tadcaster, Yorkshire, northern England, one of 26 sites monitored within the NERC Land–Ocean Interaction Study (Leeks *et al.*, 1997; Lawler *et al.*, 1999). The Wharfe site is one of five instrumented with PEEP-3 TCT sensors, three of which were estuarine sites (Lawler *et al.*, 2001). Drainage basin area at Tadcaster is 818 km^2 (Webb *et al.*, 1997), and the basin is rural and

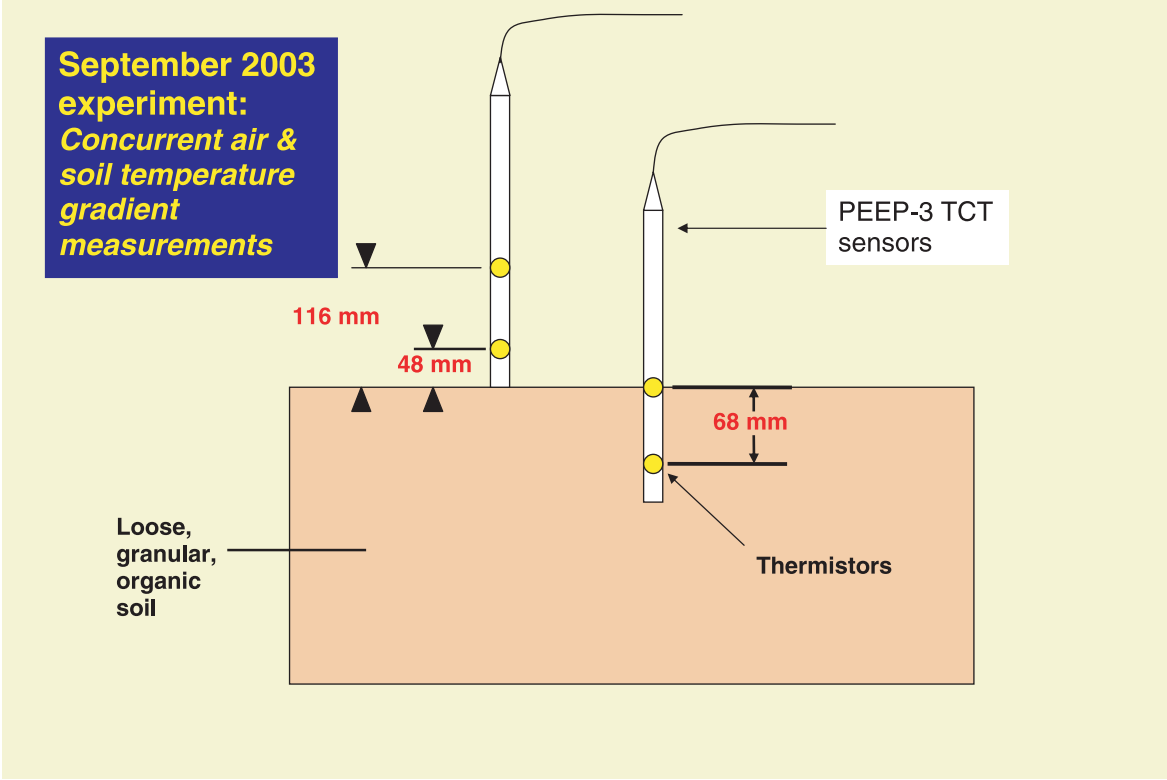

Figure 7. A simple soil erosion simulation experiment to compare temperature gradients in soil and overlying air column. This figure is available in colour online at www.interscience.wiley.com/journal/espl

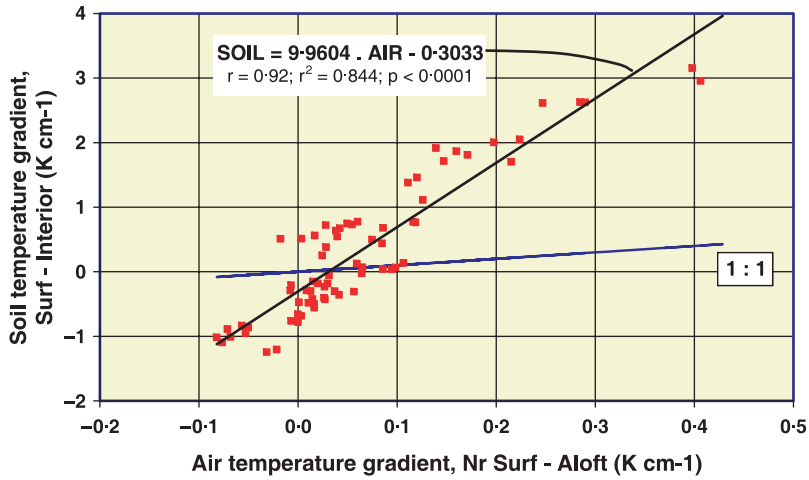

Figure 8. Relationship of vertical soil thermal gradients to vertical air thermal gradients in the simple soil erosion simulation, Warwickshire, UK, 4–11 September 2003. This figure is available in colour online at www.interscience.wiley.com/journal/espl

humid cool temperate (Jarvie *et al.*, 1997; Lawler *et al.*, 1999). Banks are >2·5 m high and materials are fine-grained with limited vegetation cover. Average annual precipitation (1961–1990) is 1139 mm, but rises to >1500 mm in the upland headwaters.

Six PEEP-3 sensors were installed horizontally at each site in a grid network to quantify key bank erosion events over a 21-month period, to generate one of the most detailed bank erosion datasets ever assembled. Erosion pins and

resurvey methods were used to pick up spatial erosion patterns. The focus here lies with example TCT and PEEP results from autumn and winter. PEEP-3 sensors were connected to a Campbell-Scientific CR10X datalogger and multiplexer scanning at 1-min intervals and storing 15-min means. This scan interval represented a balance between temporal precision and data redundancy, though higher resolution logging can be used if required. Example data are drawn from two upper-bank PEEP-3 sensors, referenced as 2U/DS (for the November event) and 4U/M (for November temperature cycling and the February erosion event). On-site stage data were generated continuously with pressure transducers: these confirmed the flow peak timings for the discharge data plotted here from the nearby Environment Agency gauging station at Tadcaster. All timings are given in GMT (Greenwich Mean Time).

Results

Diurnal bank temperature cycles

Figure 9 displays surface and subsurface river bank temperature, horizontal temperature differences, and diurnal PEEP radiation data for the Easedike site on the River Wharfe for an example 5·5-day period in autumn (1–6 November) from PEEP-3 (ref. 4U/M). This period of stable banks and low-flow conditions, punctuated by modest stage rises, none of which reached the PEEP position, included a mixture of warm days of high insolation either side of a cool, dull day (2 November; Figure 9). Incoming radiation is indexed by the PEEP-3 reference cell signal, and temperatures by the two thermistor series in Figure 9. The warm days are characterized by relatively rapid bank heating, driven by strong early-morning radiation inputs. Interestingly, Figure 9 also suggests that many features of soil thermal dynamics theory seem to be replicated at this bank site, especially classic diurnal temperature cycling behaviour (Figures 1–4 and 9). For example, the bank interior shows a more damped diurnal cycle than the bank surface, especially for maxima, even on the overcast day (Figure 9). Temperature differences (TD) between bank surface and interior range from −2 K to more than 7·5 K, and tend to peak just before maximum radiation receipt. The TD series crosses the zero line at approximately a semi-diurnal frequency as anticipated (Figure 9), but these are transient events and interfere very little with TCT methodologies which depend on the identification of sustained and constant low temperature differences (thermal consonance). The example results presented in Figure 9 represent conditions which,

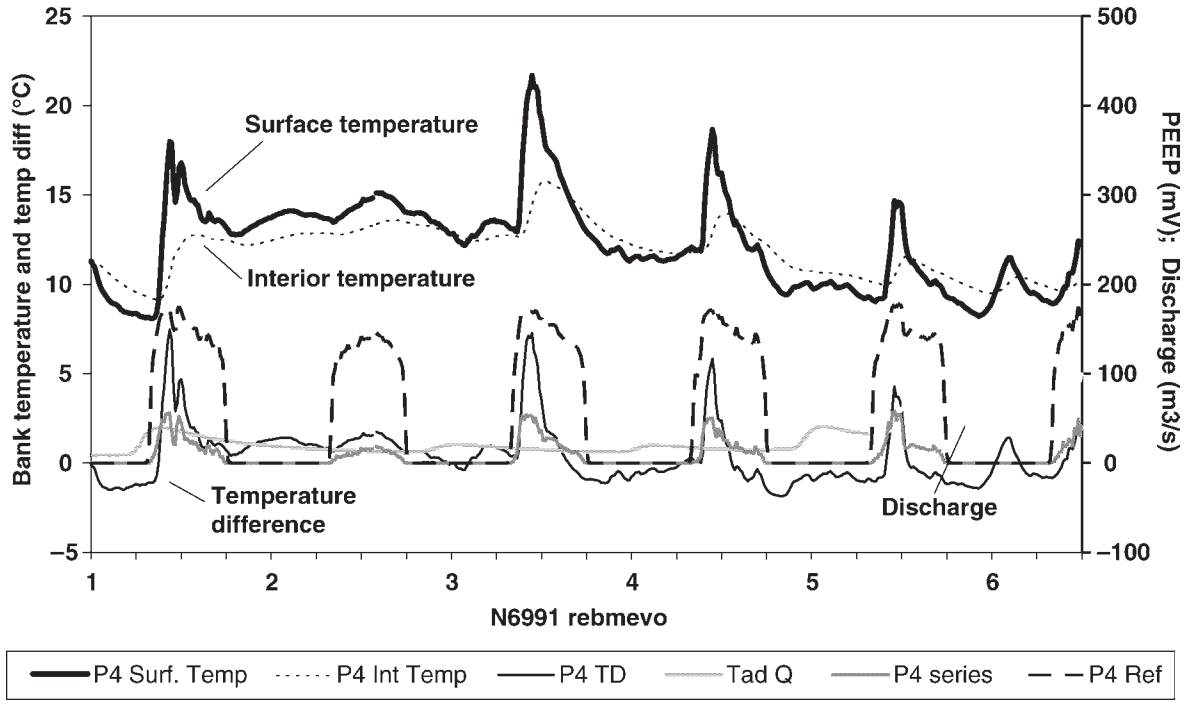

Figure 9. Diurnal patterns of river bank temperature response to on-site radiation inputs for 1–6 November 1996 at Easedike, River Wharfe, Yorkshire, UK (PEEP-3 ref. 4U/M). Temperature differences are measured horizontally into the bank.

although far from ideal for the development of bank temperature gradients, with modest radiation inputs associated with autumn, are entirely sufficient for TCT purposes, as discussed below.

Erosion event 1: November

Some example results, drawn from two flow events of dissimilar magnitude and antecedent conditions occurring under different synoptic situations in late autumn and late winter, and driving different bank responses, will demonstrate the usefulness of the TCT approach in defining more clearly, over a reasonable range of conditions, the timing of erosion events in relation to the hydrograph. The first event, in November 1996, is shown in Figure 10 where the typical diurnal output sequence generated by a second PEEP-3 sensor (ref. 2U/DS) can be seen. Reference cell signals peak at *c.* 150–175 mV each day, but fall to 0 mV each night. In response to a very high, relatively short-lived flow event on 6–7 November, however, the PEEP cell series data confirm that an erosion event occurred (Figure 10). The magnitude of the erosion event is >150 mm (as it exceeded the remaining range of that particular PEEP sensor). The maximum outputs from the second, back reference cell at the interior end of the photovoltaic cell array, also confirm that the complete active length of the PEEP-3 sensor has been exposed to light (Figure 10).

The PEEP erosion 'event window', in which the incident took place is 18 h long, and runs from 14:15 hours on 6 November to 08:15 hours on 7 November (Figure 10). Although such information usefully associates erosion with the hydrograph, it is impossible to tell from these particular PEEP data, collected during low- or zero-light conditions under nocturnal or submerged conditions, whether erosion occurred during or after the flow event (Figure 10). This can be important diagnostically for process inference: for example, it has been hypothesized that mass failure events occur more frequently on falling limbs or after the hydrograph, because of pore water pressure time-lags, reduction on matric suction and/or removal of transient bank support provided by lateral hydrostatic confining pressures (e.g. Lawler and Leeks, 1992; Lawler *et al.*, 1997b; Simon *et al.*, 2000; Rinaldi *et al.*, 2004).

Refining erosion timing with TCT approaches

Application of the new TCT approach, however, now allows us to refine the timing much more precisely and to begin to address a key question: when does erosion take place relative to the hydrograph? Note in Figure 10 that the bank surface temperature (T_s) time series for 1–5 November has a much higher amplitude than the interior temperature (T_i) time series, which is a key characteristic of soil thermal response (e.g. Cellier *et al.*, 1996), and of the other PEEP-3 sensor bank position considered in Figure 9. However, during the flow event on 6 November, the T_s and T_i time series suddenly become virtually identical (thermally consonant), suggesting that a sustained quasi-isothermal condition driven by erosion has been achieved (Figure 10). This is more clearly seen in the temperature difference time series in Figure 10. Note that temperature differences become constant and near-zero ($-0{\cdot}3\ \mathrm{K} < \mathrm{TD} < +0{\cdot}3\ \mathrm{K}$) at 15:00 hours on 6 November: this begins 1·5 h after inundation, and 2 h before the discharge peak (Figure 10). TCT suggests, therefore, that at least 68 mm of the >150 mm bank erosion which 'exposed' both thermistors was achieved during the 8 h inundation period centred on the flow peak and, from comparisons with non-eroding TCT sites (e.g. PEEP-3 ref 4U/M), probably as a rising limb event. Fluvial processes cannot be excluded here, therefore, because retreat occurred during submergence. Subsequent field inspection confirmed a smoothed, 'planed' bank, characteristic of fluid entrainment processes.

We can also examine the horizontal TD standard deviation series, which is perhaps even more striking: note in Figure 10 how the 1 h standard deviation, calculated from four 15 min readings, abruptly reduces to near-zero at the same time as thermal consonance is achieved. Thus there are two mutually supportive ways in which the TCT approach can be applied: visual comparisons of the surface and interior temperature series, and analysis of the differenced time series; and detection of change in the statistical properties of the time series (e.g. standard deviation). Both involve minimal signal processing, and both are linked by the need to identify *sustained* change, such as persistent reduction of temperature differences to constant and near-zero levels ($<0{\cdot}3$ K here, or gradients $<0{\cdot}044\ \mathrm{K\ cm^{-1}}$). In practice, these can be distinguished from the *transient* periods of low temperature differences which happen occasionally, such as during isothermal 'crossover' points which may occur at a semi-diurnal frequency, or under prolonged inundation. Similarly, the occasional blips in the TD time series which follow the TCT point are small and short-lived, and clearly related to transient warming events (e.g. Figures 10 and 11).

Erosion event 2: February

In February 1997 a compound flow event sequence occurred at Easedike composed of three hydrographs, of similar moderate magnitude and extended base times, over a 5-day period beginning 18 February, but following a large

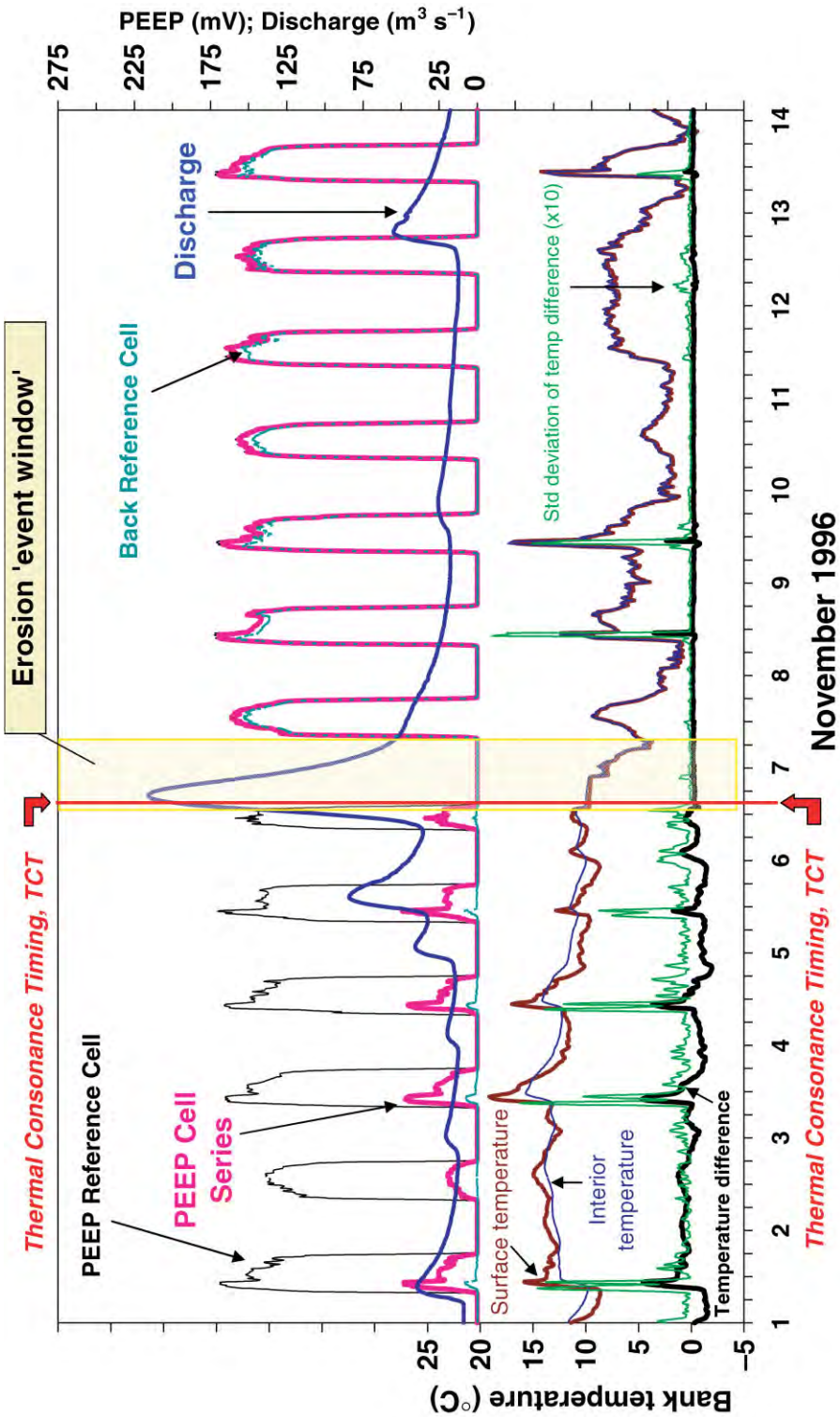

Figure 10. Bank erosion event at Easedike, River Wharfe, November 1996, in relation to flow and bank temperature time series for PEEP-3 ref. 2U/DS. This shows the application of the principle of thermal consonance timing (TCT) to fix the time of the erosion event to the inundation period, with the inference that fluvial processes cannot be excluded. Temperature differences are measured horizontally into the bank. This figure is available in colour online at www.interscience.wiley.com/journal/espl

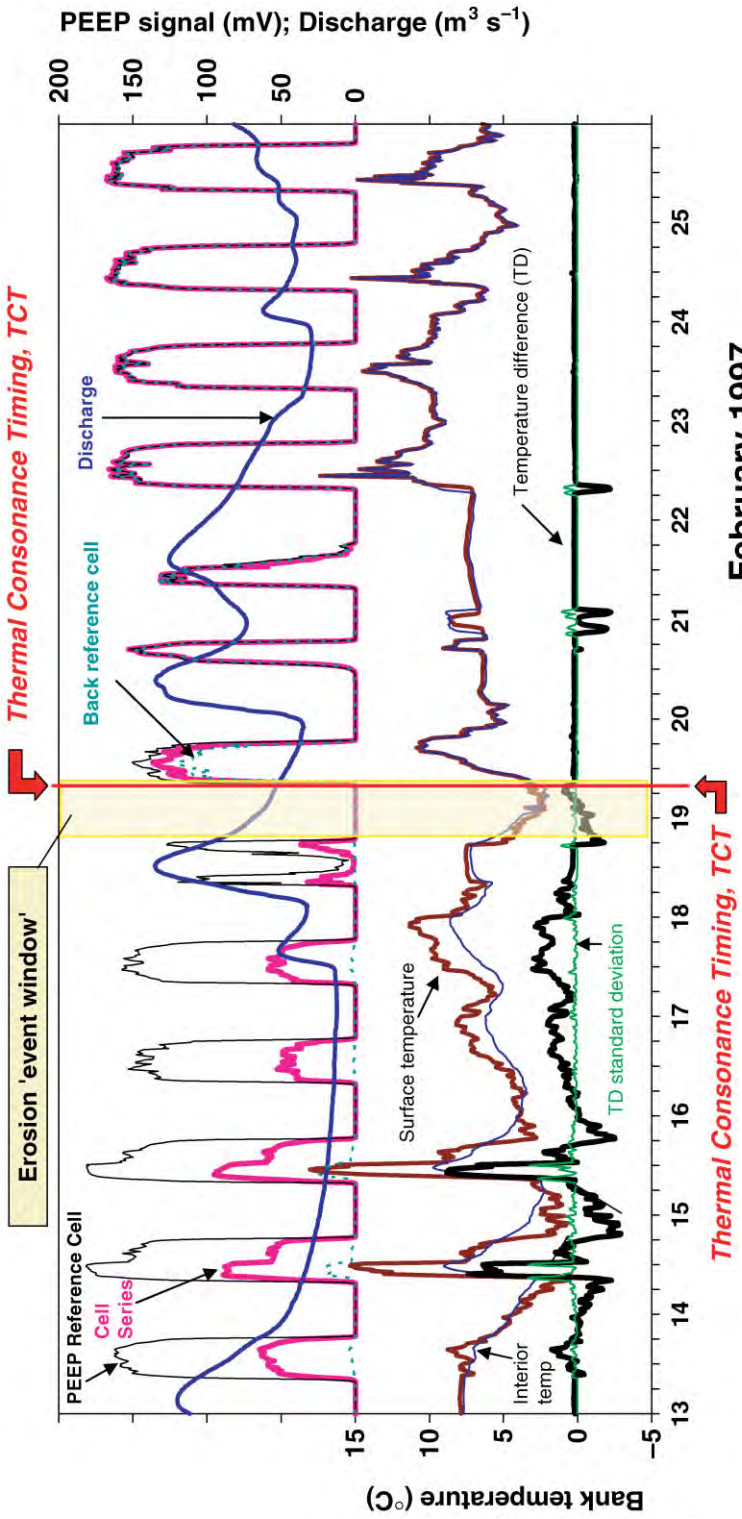

Figure 11. Bank erosion event at Easedike, River Wharfe, February 1997, in relation to flow and bank temperature time series (PEEP-3 ref. 4U/M). This shows the application of the principle of thermal consonance timing (TCT) to fix the time of the erosion event to 19 h after the discharge peak, and 13 h after re-emergence from the flow, suggesting a mass failure process (see Figure 12 also). Temperature differences are measured horizontally into the bank. This figure is available in colour online at www.interscience.wiley.com/journal/espl

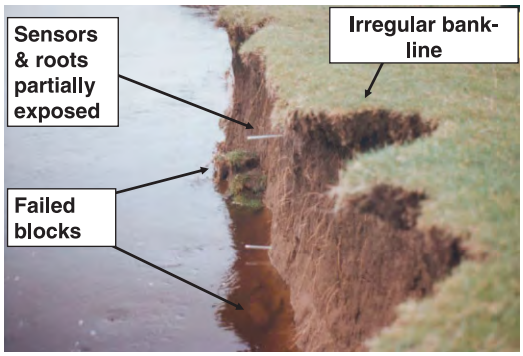

Figure 12. Evidence of mass failure at the Easedike site photographed eight days after the bank erosion event of Figure 11, including failed bocks at the bank toe. This figure is available in colour online at www.interscience.wiley.com/journal/espl

precursor flow event on 13 February (Figure 11). The change in upper bank PEEP-3 (4U/M) cell series outputs evident on 19 February confirmed that bank erosion of 140 mm had occurred since the previous day (Figure 11). The PEEP-3 back reference cell signal also increases substantially, which reconfirms significant bank erosion (Figure 11). The PEEP erosion event window lasts for 13·5 h, running from 19:00 hours on 18 February to 08:30 hours on 19 February, placing it on the hydrograph recessional limb (Figure 11). TCT evidence, however, fixes the precise timing to 08:15 hours on 19 February, towards the end of the erosion event window (Figure 11). This is also supported by the 1 h standard deviation time series, which drops by an order of magnitude at this time (Figure 11). This clearly times the erosion event to the end of the recessional limb of the first hydrograph event, 19 h after the discharge peak (Figure 11), and 13 h after emergence from the flow.

Process inference

Trying to identify the retreat process(es) or process groups responsible, from a multiplicity of possible mechanisms operating on river banks, is difficult (Lawler, 1992; Lawler *et al.*, 1997a), but erosion event timing information can provide key diagnostic evidence. The important conclusion from the February example is that a bank erosion event has been detected, confirmed to be a delayed retreat phenomenon, and the time-lag quantified. Delayed bank retreat events such as this one, 13 h *after* emergence from the water, suggest that direct fluid entrainment is not the primary erosion process in this case.

An alternative inference is that mass failure was the process involved. Extremely limited quantitative data on delayed erosion exist in the literature (but see Lawler and Leeks, 1992; Simon *et al.*, 2000; Rinaldi *et al.*, 2004), although some anecdotal evidence is available. A time-lag between peak flow and bank retreat can be indicative of mass failure (e.g. Lawler and Leeks, 1992; Lawler *et al.*, 1997b; Simon *et al.*, 2000), which may be delayed until the lateral confining support provided by the floodwaters themselves is withdrawn and/or pore water pressures have risen to critical levels, or matric suction has been destroyed (e.g. Dapporto *et al.*, 2003; Rinaldi *et al.*, 2004). Interestingly, Figure 12, taken 8 days after the February flow event, shows the classic signs of mass failure, with an irregular rather than 'planed' bankline, and failed blocks at the bank toe. The failure may have been assisted by the precursor flow event on 13 February (Figure 11), which may have raised bank pore water pressures to near-critical levels prior to the main event, as found by Rinaldi *et al.* (2004) in Tuscan river banks. We know from PEEP and TCT data that this antecedent flood did not lead to bank retreat directly (Figure 11), and was therefore a subcritical event. This demonstrates, therefore, the utility of TCT and PEEP approaches in confirming stability in the face of potentially destabilizing forces, which is useful for threshold definition (e.g. critical flow levels, inundation durations or shear stresses required for erosion). Though further testing is needed under a range of conditions time lags appear to be quite accurately and routinely quantifiable with TCT, opening up the exciting possibility of rigorous and longer-term validation of geotechnical stability and hydrodynamic models which predict failure in relation to critical conditions (e.g. Darby and Thorne, 1996; Darby, 2000; Mosselman, 2000; Simon *et al.*, 2000; Rinaldi *et al.*, 2004).

Quasi-instantaneous bank erosion

It appears that the February event was achieved within the 15 min logger scan interval, i.e. it was quasi-instantaneous. This is a significant result, and suggests that bank retreat was at least partly a 'catastrophic' rather than 'progressive'

phenomenon. Also, the November event took place during inundation, while the February event followed emergence, suggesting mass failure. This raises the possibility of testing for intra-event, inter-event, subseasonal or seasonal change in rates and driving processes of bank erosion using TCT. The idea of 'catastrophic retreat' may mean that conventional views (e.g. excess boundary shear stress approaches, where erosion is assumed to continue at a progressive rate proportional to stress for as long as supercritical conditions obtain) may need revisiting. Discriminating between 'catastrophic retreat' and 'progressive entrainment' may now be possible, and represents an interesting future research direction for fluvial and non-fluvial systems, especially the definition of shifting critical entrainment or geotechnical stresses required.

Discussion: Prospects and Research Needs

Developing the TCT principle

The TCT concept can offer further opportunities throughout geomorphology to address the seven challenges established in the Introduction: the discussion below, however, focuses largely on fluvial applications. Erosion event magnitude and timing information, which is crucial to process inference, can now be defined in a mutually supportive way, based on two different measurement principles: light (conventional PEEP methodologies) and heat (TCT approaches). Encouragingly, both the November and February erosion events are timed by TCT methods to lie within the longer erosion event window fixed by conventional PEEP data (Figures 10 and 11). Though further testing is desirable, the examples here show the considerable potential of the TCT approach, even with preliminary instrumentation and site conditions (fine-grained materials subject to regular inundation, in the autumn–winter period within a cool temperature climate zone) which were far from ideal. Warmer, drier environments with sandy materials where sediment temperature gradients are maximized are likely to be especially appropriate (e.g. coastal or desert dunes, arroyos, mountain gullies). Future work will focus on analysis of the much-neglected controls of river bank thermal regimes (Figure 9), and the development of a dedicated TCT sensor equipped with multiple thermistors in sensitive bridge circuits: both foci will assist application of the principle to a range of geomorphological contexts, sites and conditions. Such a system may help to shed light on riparian wetting front movement and moisture fluxes, which are critical to bank stability (e.g. Lawler *et al.*, 1997a; Darby, 2000; Simon *et al.*, 2000; Dapporto *et al.*, 2003; Rinaldi *et al.*, 2004), in much the same way that thermal studies have achieved for groundwater exchanges in the hyporheic zone (e.g. Evans and Petts, 1997).

Field verification of process–response models

Rigorous field verification of high resolution process–response models is likely to be a key area for future geomorphological research. However, Lawler (1992) argued that the lack of an appropriate field validation method to test and improve erosion models was a key problem area hindering progress in such a complex field, where subaerial, hydrodynamic, geotechnical, geochemical and biological processes combine. Darby (2000, p. 340), too, notes: 'comparisons between simulated and observed bank erosion rates are somewhat difficult to make, since observed bank erosion rates are based on a 20-year average for the simulation period, rather than rates for the shorter time-spans over which event-driven erosion rates operate'. Distributed TCT approaches offer substantial potential here for the field evaluation of erosion rate and process models (e.g. Darby and Thorne, 1996; Darby, 2000; Mosselman, 2000; Rinaldi *et al.*, 2004). It is perhaps now timely to launch combined investigations which integrate terrestrial photogrammetric monitoring, to give excellent spatial data (e.g. Lawler, 1989; Lane *et al.*, 1993; Westaway *et al.*, 2000; Brasington *et al.*, 2003), with TCT approaches at several strategic points to provide the key dynamics information of event magnitude, timing, duration and frequency at the required temporal resolution. Thus, a key research need now is to integrate at appropriate spatial and temporal scales (1) the new generation of finely resolved process models (e.g. Bates and Lane, 2000) with (2) high temporal resolution, event-based, field validation approaches, (3) high-resolution spatial monitoring of landforms, and (4) simultaneous analysis of the driving forces.

Process inference, hypothesis discrimination and threshold identification

In episodic geomorphological systems, sound process work often depends on capturing erosion and deposition event magnitudes, timings, durations and frequencies. It now appears possible with TCT to obtain erosion rate details (L/T in dimensional terms) which are closer to actual values, because (a) event timing and duration (T) is more accurately identified between temporal boundary conditions, and (b) L (retreat distances) are event-based, rather then temporally

lumped, values. This is especially helpful in highly dynamic environments or scour-and-fill-dominated systems such as semi-arid or tidal channels, or dune systems, where erosion can be concealed by later accretion, and could usefully build on earlier PEEP investigations (e.g. Lawler, 1994; Mitchell *et al.*, 1999; Stott, 1999; Prosser *et al.*, 2000; Lawler *et al.*, 2001). More robust event-based rate information provides a stronger platform for the discrimination of process-dominance hypotheses (e.g. Lawler, 1992). Arguably, for example, bank erosion could be hypothesized to peak on rising limbs if preparation processes were important, but on or after recessional limbs if mass failure was dominant, because of lags involved in pore water pressure increases and removal of lateral confining pressures (e.g. Lawler and Leeks, 1992; Lawler *et al.*, 1997a; Simon *et al.*, 2000; Rinaldi *et al.*, 2004), as for the February event here (Figure 11). Similarly, it is likely that TCT data can help to eliminate certain controlling processes because of event precedence issues, i.e. at its simplest level, TCT can establish a temporal boundary condition to the erosion problem, because potential forcing events which occur *after* the timed erosional activity cannot be directly responsible for the erosion recorded. Moreover, because the moment of erosion can be better identified in relation to transient fluctuations in the driving forces, TCT should be able to define more clearly shifting system thresholds (e.g. critical pore water pressures or boundary shear stresses). Such bank stability criteria are considered crucial to the explanation of alluvial channel form (e.g. Eaton *et al.*, 2004). The TCT concept can also confirm stability in the face of potentially erosive events, information which, arguably, is equally fundamental to threshold definition (e.g. Figure 11; 13 February event).

Understanding the controls and implications of sediment thermal response

TCT approaches can assist understanding of landform thermal responses because they capture on-site, high-resolution sediment temperature gradient data. Though neglected, these are important indices in their own right for: preconditioning processes, such as desiccation (Cameron, 2001), freeze–thaw (e.g. 13 November event in Figure 10: see also Lawler, 1986, 1993b; Branson *et al.*, 1996), and sediment hydration (Dapporto *et al.*, 2003); hydraulic behaviour of sediments (e.g. Romero *et al.*, 2001); cohesive sediment erosion; perifluvial energy and moisture balances and fluxes (e.g. Evans *et al.*, 1998; Hankin *et al.*, 2002); vegetation growth, seed germination and riparian habitats; and geochemical and hydrochemical processes. The radiation data captured by PEEP-3 sensors can also help to explain thermal processes and interpret on-site biological processes, including erosionally relevant ones (e.g. vegetation growth). It is also possible to use derived thermal gradient data to help estimate sediment heat flux rates (e.g. Oke, 1987; Cellier *et al.*, 1996; Ogée *et al.*, 2001).

Event-based sediment dynamics investigations

Field validation of sediment flux dynamics models (e.g. Mosselman, 2000) should now be more achievable at event timescales, to build on temporally aggregated studies (e.g. Ashbridge, 1995). For example, TCT approaches should help to establish links between fluvial sediment flux and the magnitude and timing of inputs of sediments, and any associated contaminants, organics and nutrients, from channel sides or elsewhere (e.g. Oostwoud Wijdenes and Bryan, 2001; Lawler *et al.*, 2003; Old *et al.*, 2005). For instance, if bank preparation processes were important, and led to widespread sediment entrainment on the rising limb, then sediment slugs could be expected early on in the hydrograph, resulting in clockwise flow-sediment hysteresis (e.g. Bogen, 1980; Walling, 1988; Walling and Webb, 1982; Lawler, 2005). The TCT principle in converse could also be used to quantify depositional event timing, duration, magnitude and rates as part of sedimentological or geomorphological studies. The lack of bank accretion research, in particular, has hindered width modelling (Mosselman, 2000), although some high-resolution tidal channel deposition and erosion rate information has now begun to emerge (e.g. Mitchell *et al.*, 1999; Lawler *et al.*, 2001; Lawler, 2005).

Conclusions

The principle of thermal consonance timing has been established to define, more accurately than with existing methods, the timing and magnitude of erosion and deposition events. TCT of erosion is based on monitoring the switch from strong temperature gradients in sediments to the weaker ones developed in air and water, which indicates sediment removal. The TCT principle draws on micrometeorological theory as applied to perifluvial zones, published empirical evidence, and results from simulations and monitoring at a River Wharfe bank erosion site. The modified PEEP-3 TCT instrument developed allows initial field TCT monitoring. River bank thermal regimes respond as classic soil temperature and energy balance theory predicts, and as soil thermal profile data confirm. The example bank temperature dynamics data presented considerably augment the very few published data available.

TCT helped to fix the magnitude and timing of two specific example erosion events. The late autumn event was timed to within a few hours of the flow peak, so that fluid entrainment processes could not be excluded. The late winter example was fixed to 19 h *after* the flow peak, and represents a rare quantified confirmation that delayed bank erosion can occur (see also Lawler and Leeks, 1992; Lawler *et al.*, 1997b; Simon *et al.*, 2000; Rinaldi *et al.*, 2004). Furthermore, because erosion occurred 13 h *after* emergence from the flow, direct fluvial process control can be relegated. Instead, TCT and photographic information suggested mass failure, and demonstrated how knowledge of response timing is crucial to process diagnostics. Furthermore, the February erosion event appears to be virtually instantaneous, suggesting 'catastrophic retreat' rather than slower 'progressive entrainment'. The general applicability of this finding deserves further attention, for it has implications for the mechanics of failure and sediment injection dynamics.

The improved information on erosion event magnitude and timing is promising, and raises exciting possibilities for developing and testing TCT approaches for a range of geomorphological process investigations and conditions, including: the derivation of closer approximations to 'true' erosion and deposition rates; field validation of high-resolution process–response models (e.g. fluid entrainment or geotechnical stability models); process inference, hypothesis discrimination and threshold identification (e.g. changing critical shear stresses required under time-varying erodibility scenarios (Lawler, 2005); improving understanding of the controls and implications of sediment thermal responses; and event-based sediment supply and flux dynamics investigations. It would also be useful to combine digital photogrammetric approaches for high-resolution spatial data, with TCT approaches which deliver finely revolved event dynamics information. The potential for application to wider erosion and deposition dynamics problems, such as gully development, hillslope erosion, arroyo scour-and-fill, sheetwash, dune deflation, and mudflat or beach erosion, appears to be considerable.

Acknowledgements

I am very grateful for funding of the field component of this study from the UK Natural Environment Research Council (Land-Ocean Interaction Study; NERC Grant GST/02/1184), field support from John Couperthwaite, Adam Sawyer, Richard Johnson, Steve Mitchell, Graham Leeks and CEH, and the UK Environment Agency, and useful comments from the referees and editor. I greatly appreciate the help with data input provided by Catherine Lawler.

References

Ashbridge D. 1995. Processes of river bank erosion and their contribution to the suspended sediment load of the River Culm, Devon, In *Changing River Channels*, Foster IDL, Gurnell AM, Webb BW (eds). John Wiley and Sons: Chichester; 229–245.

Barker R, Dixon L, Hooke J. 1997. Use of terrestrial photogrammetry for monitoring and measuring bank erosion. *Earth Surface Processes And Landforms* **22**: 1217–1227.

Bates PD, Lane SN (eds). 2000. *High-Resolution Flow Modelling in Hydrology and Geomorphology*, John Wiley and Sons: Chichester.

Betteridge KFE, Williams JJ, Thorne PD, Bell PS. 2003. Acoustic instrumentation for measuring near-bed sediment processes and hydrodynamics. *Journal of Experimental Marine Biology and Ecology* **285**: 105–118.

Bogen J. 1980. The hysteresis effect of sediment transport systems. *Norsk Geografiska Tidsskrift* **34**: 45–54.

Branson J, Lawler DM, Glen JW. 1996. Sediment inclusion events during needle-ice growth: a laboratory investigation of the role of soil moisture and temperature fluctuations. *Water Resources Research* **32**: 459–466.

Brasington J, Langham J, Rumsby B. 2003. Methodological sensitivity of morphometric estimates of coarse fluvial sediment transport. *Geomorphology* **53**: 299–316.

Cameron DA. 2001. The extent of soil desiccation near trees in a semi-arid environment. *Geotechnical and Geological Engineering* **19**: 357–370.

Casadei M, Dietrich WE, Miller NL. 2003. Testing a model for predicting the timing and location of shallow landslide initiation in soil-mantled landscapes. *Earth Surface Processes and Landforms* **28**: 925–950.

Cellier P, Richard G, Robin P. 1996. Partition of sensible heat fluxes into bare soil and the atmosphere. *Agricultural and Forest Meteorology* **82**: 245–265.

Church M. 1980. Records of recent geomorphological events. In *Timescales in Geomorphology*, Cullingford RA, Davidson DA, Lewin J (eds). John Wiley and Sons: Chichester; 13–29.

Church M. 1996. Space, time and the mountain – how do we order what we see? In *The Scientific Nature of Geomorphology*, Rhoads BL, Thorn CE (eds). *Proceedings of 27th Binghampton Symposium in Geomorphology*. John Wiley and Sons: Chichester; 147–170.

Couperthwaite JS, Mitchell SB, West JR, Lawler DM. 1998. Cohesive sediment dynamics on an inter-tidal bank on the tidal Trent, UK. *Marine Pollution Bulletin* **37**(3–7): 144–154.

Dapporto S, Rinaldi M, Casagli N, Vannocci P. 2003. Mechanisms of riverbank failure along the: Arno River, Central italy, *Earth Surface Processes and Landforms* **28**: 1303–1323.

Darby SE. 2000. Modelling width adjustment in straight alluvial channels. In *High-Resolution Flow Modelling in Hydrology and Geomorphology*, Bates PD, Lane SN (eds). John Wiley and Sons: Chichester; 325–347.

Darby SE, Thorne CR. 1996. Development and testing of riverbank-stability analysis. *Proceedings of the American Society of Civil Engineers, Journal of Hydraulic Engineering* **122**: 443–454.

Eaton BC, Church M, Millar R. 2004. Rational regime model of alluvial channel morphology and response. *Earth Surface Processes and Landforms* **29**: 511–529.

Evans EC, Petts GE. 1997. Hyporheic temperature patterns within riffles. *Hydrological Sciences Journal* **42**: 199–213.

Evans EC, McGregor GR, Petts GE. 1998. River energy budgets with special reference to river bed processes. *Hydrological Processes* **12**: 575–595.

Garcia C, Laronne JB, Sala M. 2000. Continuous monitoring of bedload flux in a mountain gravel-bed river. *Geomorphology* **34**: 23–31.

Habersack HM, Nachtnebel HP, Laronne JB. 2001. The continuous measurement of bedload discharge in a large alpine gravel bed river, *Journal of Hydraulic Research* **39**: 125–133.

Hall K. 2004. Evidence for freeze-thaw events and their implications for rock weathering in northern Canada. *Earth Surface Processes and Landforms* **29**: 43–57.

Hankin BG, Holland MJ, Beven KJ, Carling PA. 2002. Computational fluid dynamics modelling of flow and energy fluxes for a natural fluvial dead zone. *Journal of Hydraulic Research* **40**: 389–401.

Jarvie HP, Neal C, Robson AJ. 1997. The geography of the Humber catchment. *Science of the Total Enviroment* **194/195**: 87–99.

Kumar P, Kaleita AL. 2003. Assimilation of near-surface temperature using extended Kalman filter. *Advances in Water Resources* **26**: 79–93.

Lane SN. 1998. The use of digital terrain modelling in the understanding of dynamic river channel systems. In *Landform Monitoring, Modelling and Analysis*, Lane SN, Richards KS, Chandler JH (eds). John Wiley and Sons: Chichester; 311–342.

Lane SN, Richards KS, Chandler JH. 1993. Developments in photogrammetry; the geomorphological potential. *Progress in Physical Geography* **17**: 306–328.

Lane SN, Chandler JH, Richards KS. 1998a. Landform monitoring, modelling and analysis: land *form* in geomorphological research. In *Landform Monitoring, Modelling and Analysis*, Lane SN, Richards KS, Chandler JH (eds). John Wiley and Sons: Chichester; 1–17.

Lane SN, Richards KS, Chandler JH (eds) 1998b. *Landform Monitoring, Modelling and Analysis*. John Wiley and Sons: Chichester.

Lantzke IR, Mitchell DS, Haritage AD, Sharma KP. 1999. A model of factors controlling orthophosphate removal in planted vertical flow wetlands. *Ecological Engineering* **12**: 93–105.

Lau YL, Droppo IG. 2000. Influence of antecedent conditions on critical shear stress of bed sediments. *Water Research* **34**: 663–667.

Lawler DM. 1986. River bank erosion and the influence of frost: a statistical examination. *Transactions of the Institute of British Geographers* **11**: 227–242.

Lawler DM. 1987. Bank erosion and frost action: an example from South Wales. In *International Geomorphology 1986, Part 1*, Gardiner V (ed.). John Wiley and Sons: Chichester; 575–590.

Lawler DM. 1989. *Some new developments in erosion monitoring: 2. The potential of terrestrial photogrammetric methods*. School of Geography, University of Birmingham Working Paper 48.

Lawler DM. 1991. A new technique for the automatic monitoring of erosion and deposition rates. *Water Resources Research* **27**: 2125–2128.

Lawler DM. 1992. Process dominance in bank erosion systems. In *Lowland Floodplain Rivers: Geomorphological Perspectives*, Carling PA, Petts GE (eds). John Wiley and Sons: Chichester; 117–143.

Lawler DM. 1993a. The measurement of river bank erosion and lateral channel change: a review. *Earth Surface Processes and Landforms* **18**: 777–821.

Lawler DM. 1993b. Needle ice processes and sediment mobilization on river banks: the River Ilston, West Glamorgan, UK. *Journal of Hydrology* **150**: 81–114.

Lawler DM. 1994. Temporal variability in streambank response to individual flow events: the River Arrow, Warwickshire, UK. In *Variability in Stream Erosion and Sediment Transport*, Olive L *et al.* (eds). International Association of Hydrological Sciences Publication **224**: 171–180.

Lawler DM. 2005. The importance of high-resolution monitoring in erosion and deposition dynamics studies: examples from estuarine and fluvial systems. *Geomorphology* **64**: 1–23.

Lawler DM, Leeks GJL. 1992. River bank erosion events on the Upper Severn detected by the Photo-Electronic Erosion Pin (PEEP) system. In *Erosion and Sediment Transport Monitoring Programmes in River Basins, Proceedings of the Oslo Symposium.* Bogen J, Walling DE, Day TJ (eds). International Association of Hydrological Scientists Publication **210**: 95–105.

Lawler DM, Thorne CR, Hooke JM. 1997a. Bank erosion and instability. In *Applied Fluvial Geomorphology for River Engineering and Management*, Thorne CR, Hey RD, Newson MD (eds). John Wiley and Sons: Chichester; 137–172.

Lawler DM, Couperthwaite J, Bull LJ, Harris NM. 1997b. Bank erosion events and processes in the Upper Severn basin. *Hydrology and Earth System Sciences* **1**: 523–534.

Lawler DM, Grove J, Couperthwaite JS, Leeks GJL. 1999. Downstream change in river bank erosion rates in the Swale-Ouse system, northern England. *Hydrological Processes* **13**: 977–992.

Lawler DM, West JR, Couperthwaite JS, Mitchell SB. 2001. Application of a novel automatic erosion and deposition monitoring system at a channel bank site on the tidal River Trent, UK. *Estuarine, Coastal and Shelf Science* **53**(2): 237–247.

Lawler DM, McGregor GR, Phillips ID. 2003. Influence of atmospheric circulation changes and regional climate variability on river flow and suspended sediment fluxes in southern Iceland. *Hydrological Processes* **17**: 3195–3223.

Leeks GJL, Neal C, Jarvie HP, Casey H, Leach DV. 1997. The LOIS river monitoring network; strategy and implementation. *Science of the Total Environment* **194/195**: 101–109.

Mitchell SB, Couperthwaite JS, West JR, Lawler DM. 1999. Dynamics of erosion and deposition events on an intertidal mudbank at Burringham, River Trent, UK. *Hydrological Processes* **13**: 1155–1166.

Mitchell SB, West JR, Couperthwaite JS, Lawler DM. 2003. Measuring sediment exchange rates on an intertidal bank at Blacktoft, Humber Estuary, UK. *Science of the Total Environment* **314/316**: 535–549.

Morris BD, Davidson MA, Huntley DA. 2001. Measurements of the response of a coastal inlet using video monitoring techniques. *Marine Geology* **175**: 251–272.

Mosselman E. 2000. Morphological modelling or rivers with erodible banks. In *High-Resolution Flow Modelling in Hydrology and Geomorphology*, Bates PD, Lane SN (eds). John Wiley and Sons: Chichester; 348–362.

Ogée J, Brunet Y. 2002. A forest floor model for heat and moisture including a litter layer. *Journal of Hydrology* **255**: 212–233.

Ogée J, Lamaud E, Brunet Y, Berbigier P, Bonnefond JM. 2001. A long-term study of soil heat flux under a forest canopy. *Agricultural and Forest Meteorology* **106**: 173–186.

Oke TR. 1987. *Boundary Layer Climates* (second edition). Methuen: London.

Old GH, Lawler DM, Snorrason A. 2005. Flow and sediment dynamics of a glacial outburst flood from the Skaftá system in southern Iceland. Earth Surface Processes and Landforms **30**: 1441–1460.

Oostwoud Wijdenes DJ, Bryan R. 2001. Gully-head erosion processes on a semi-arid valley floor in Kenya: a case study into temporal variation and sediment budgeting. *Earth Surface Processes and Landforms* **26**: 911–933.

Prosser IP, Hughes AO, Rutherfurd ID. 2000. Bank erosion of an incised upland channel by subaerial processes: Tasmania, Australia. *Earth Surface Processes and Landforms* **25**: 1085–1101.

Richards K. 1996. Samples and cases: generalisation and explanation in geomorphology. In *The Scientific Nature of Geomorphology: Proceedings of the 27th Binghampton Symposium in Geomorphology*, Rhoads BL, Thorn CE (eds). John Wiley and Sons: Chichester; 171–190.

Ridd P, Day G, Thomas S, Harradence J, Fox D, Bunt J, Renagi O, Jago C. 2001. Measurement of sediment deposition rates using an optical backscatter sensor. *Estuarine, Coastal and Shelf Science* **52**: 155–163.

Rinaldi M, Casagli N, Dapporto S, Gargini A. 2004. Monitoring and modelling of pore water pressure changes and riverbank stability during flow events. *Earth Surface Processes and Landforms* **29**: 237–254.

Romero E, Gens A, Loret A. 2001. Temperature effects on the hydraulic behaviour of an unsaturated clay. *Geotechnical and Geological Engineering* **19**: 311–332.

Simon A, Castro J. 2003. Measurement and analysis of alluvial channel form. In *Tools in Fluvial Geomorphology*, Kondolf GM, Piegay H. (eds). John Wiley and Sons: Chichester; 291–322.

Simon A, Curini A, Darby SE, Langendoen EJ. 2000. Bank and near-bank processes in an incised channel. *Geomorphology* **35**: 193–217.

Sinokrot BA, Stefan HG. 1993. Stream temperature dynamics: measurements and modeling. *Water Resources Research* **29**: 2299–2312.

Stott T. 1999. Stream bank and forest ditch erosion: preliminary responses to timber harvesting in mid-Wales. In *Fluvial Processes and Environmental Change*. Brown AG, Quine TA (eds). John Wiley and Sons: Chichester; 47–70.

Walling DE. 1988. Erosion and sediment yield research – some recent perspectives. *Journal of Hydrology* **100**: 113–141.

Walling DE, Webb BW. 1982. Sediment availability and the prediction of storm period sediment yields. In *Fluvial Processes and Environmental Change, Recent developments in the explanation and prediction of erosion and sediment yield*, Walling DE (ed.). International Association of Hydrological Sciences Publication No. 137: 327–337.

Webb BW, Zhang Y. 1999. Water temperatures and heat budgets in Dorset chalk water courses. *Hydrological Processes* **13**: 309–321.

Webb BW, Phillips JM, Walling DE, Littlewood IG, Watts CD, Leeks GJL. 1997. Load estimation methodologies for British rivers and their relevance to the LOIS RACS programme. *Science of the Total Environment* **194/195**: 87–99.

Westaway RM, Lane SN, Hicks DM. 2000. The development of an automated correction procedure for digital photogrammetry for the study of wide, shallow, gravel-bed rivers. *Earth Surface Processes and Landforms* **25**: 209–226.

